A MODEL TO SIMULATE EM SWITCHING TRANSIENTS IN ELECTRIC POWER DISTRIBUTION SUBSTATIONS

G. Ala, P. Buccheri, M. Inzerillo
Dipartimento di Ingegneria Elettrica - Universitˆ di Palermo
Viale delle Scienze, 90128 Palermo (Italia)
Tel : +39 091 6566258 - Fax : +39 091 488452 - E-mail : ala@diepa.unipa.it

ABSTRACT

Switching transients are the main causes of electromagnetic interference with control and monitoring equipment in electric power MV/LV substations; so circuit-breakers have to be taken into account as EMI sources. In the paper a numerical model is presented to calculate transient electric and magnetic fields due to switching operation. The simulation is based on the use of the ATP-EMTP and of a code using a field approach based on the method of moments. Simulation examples are carried out also underlining the shielding effects of metallic cabinets enclosing equipment which are sensitive to EM noises.

INTRODUCTION

Electronic equipment has become an integrated part of the electric power substation control system. In particular semiconductors devices are widely used in control and monitoring systems [1]. Electronic devices enable compact sizes, ease in handling and high efficiency of the systems. On the other hand, they increase the susceptibility to noise of the whole system and reduce the immunity against the electromagnetic interference (EMI).
The massive use of compact-sizes prefabricated electric power MV/LV substations, with integrated diagnostic electronic equipment and control apparatus, makes some more critical the electromagnetic compatibility (EMC) of the whole system to transients.
EMI can arise from any operation that interrupts or changes an electrical current. Hence operations of circuit-breakers and disconnectors are primary causes of EMI in power systems [2].
Transient bus currents and electromagnetic fields of significant amplitude and frequency content can arise when switchgears are operating and can interfere with control and protection equipment causing failures or misoperations. In particular the electric field is proportional to the charge transient on the bus-bar system, while the magnetic field strictly depends on the current transient. These transient currents and charges are conditioned by the nonlinear behaviour of the arc-conductance in the switch device, as well as by the reignition and the resonance phenomena, which usually give rise to distortion in wave shapes and to high frequency voltage oscillations.
The major source of EMI is the bus-bar system which works as an antenna so determining electromagnetic coupling with control and monitoring equipment. The geometry of the substation determines the dominating frequencies of the interference and the intensity of the coupling [3], [4].
EMIs associated to transient switching operations, also in short-circuit conditions, are usually considered as inevitable and unremovable events of the electromagnetic environment of MV/LV substations and so no tests have to be done in order to evaluate their emission and immunity characteristics (Standards EN 60947-1/A 11 and EN 60439-1/A 11).
In authors' opinion this EMC problem needs to be more deeply investigated in order to avoid failures or misoperations of monitoring equipment in substations.
Few existing technical papers deal with the electromagnetic interference problems in the switchgear environment of HV electric power substations, also reporting measurements performed in air/gas-insulated HV substations or HV converter stations [3], [4] [5], [6]; within the authors' knowledge, no EMI prediction model dealing with MV/LV substations environment is presented in technical literature.
On the other hand, in order to assure immunity of electronic equipment against the electromagnetic transients, one has to understand and characterize their generation, propagation and coupling mechanisms and threat levels to the substation equipment.
In this paper, a computational procedure to predict electric and magnetic fields due to switching operations in electric power MV/LV substations is illustrated, taking into account a realistic MV circuit-breakers model [7]; transient electric and magnetic fields caused by these operations are computed [8]. The way of taking into account the shielding capability of metallic enclosures of control and measurement equipment is also suggested and investigated.

SUBSTATION SIMULATION

The first step in evaluating the electric and magnetic fields produced during switching operations, is to obtain the transient voltage and current time profiles in the bus-bar system. These quantities are strictly depending on nonlinear behaviour of the arc-conductance as well as on the arrangement of the bus bar and apparatus and on load or fault conditions.
In the paper the ATP code is used to evaluate in time domain the transient voltage and current profiles of a real arc during switching operations.
The substation apparatus (bus-bars, ingoing and outgoing distribution lines) are simulated in ATP code, including a time-variable arc conductance model.
In the paper a model of circuit-breakers written in the MODELS language for ATP code is used. Each phase of the three-phase circuit-breaker is simulated by means of two series-connected ohmic resistors, whose conductance is represented by the variable arc-conductance obtained from the combination of the Mayr's and Cassies's differential arc-equations.

The following differential equation is related to the Mayr's model of the arc conductance:

$$\frac{dg_m(t)}{dt} = \frac{1}{\tau_m}\left(\frac{i^2(t)}{P_0} - g_m(t)\right) \qquad (1)$$

while the Cassie's differential model is described by the following equation:

$$\frac{dg_c(t)}{dt} = \frac{1}{\tau_c}\left(\frac{i^2(t)}{u_c \cdot g_c} - g_c(t)\right) \qquad (2)$$

where i(t) is the phase current of the circuit-breaker, g_m or g_c is the arc-conductance, $_m$ or $_c$ is the time constant of the arc; P_0 is the steady-state power loss of the arc and u_c is the steady-state arc voltage.

The total arc-conductance g is given by:

$$\frac{1}{g} = \frac{1}{gm} + \frac{1}{g_c} \qquad (3)$$

Tests prove that Mayr's model fits the arc behaviour in about ten times of microseconds close to current zero, whereas Cassie's model fits the conductance behaviour at high current, such as at the beginning of the opening operation. The following parameters of the arc model have been employed: $_m$=0.22 s, $_c$=0.8 s, P_0=8.8 kW and u_c=2.35 kV, that are related to a SF_6 MV circuit breaker [7].

In order to evaluate the electric and magnetic fields in the substation environment, a thin-wires structure is employed. A modified version of the thin-wire electric field integral equation (EFIE) is numerically solved by an authors' code by using the method of moments (MOM) in frequency domain for the structure subdivided in a number of short segments [9], [10], [11]. For the presence of a grounding mesh, the ground surface is considered perfectly conductive and the image principle is applied for each subsegments. The arc branch is modelled for each phase as a radiating segment having known time profiles both for current and voltage, so phase conductors and bus-bars are considered as radiating antennas excited by the previous branches. Thin metallic walls of cabinets containing electronic apparatus can be also simulated by means of a wire-grid subdivided in a number of short segments.

Electric and magnetic fields in any point of the substation environment can be calculated as functions of the computed longitudinal currents in the segments of the thin wires [8]. The time profiles are evaluated via discrete fast Fourier transform (DFFT). The shielding capability of the metallic enclosure of the control and measurement equipment can be evaluated.

Unlike many technical papers that consider, in other electromagnetic environment, the arc branch as a short-circuit non radiating element excited only by a current source, the authors' opinion is that both transient electric quantities, arc current and voltage, are necessary in order to carefully calculate EM radiated fields, because high frequency oscillations in the transient E-field, due to arc-voltage, take also place during switching operations.

The start point is the well known relation which expresses the total electric field:

$$E^T = E^{sc} + E^{inc} \qquad (4)$$

The E^{inc} field is the eventually existing incident field or a field imposed by the operator to carry out specific input conditions; the E^{sc} field (scattered E-field) is expressed by means of the retarded magnetic vector potential A and the retarded electric scalar potential due to all longitudinal currents and all surface charges of the structure, respectively:

$$E^{sc} = -(j\omega A + \nabla\Phi) \qquad (5)$$

By employing the thin-wire approximation, the authors choose the following integral constraint between two matching points on the generatrix of the wires which simulate the substation bus-bars:

$$-j\omega\int_{l_s} A_{tg}\cdot dl_s + \Phi_1 - \Phi_2 = z_s\int_{l_s} I_s\cdot dl_s - \int_{l_s} E_{tg}^{inc}\cdot dl_s \qquad (6)$$

where z_S is the surface impedance per unit length of a cylindrical wire.

In segments simulating the bus-bars, the last term of the right side is null; in those that simulate the circuit-breaker in its geometrical position, the first term is null and the second one is replaced by the known arc voltage in the right member of the previous equation.

By applying the direct method of moments via point matching procedure, a discrete formulation of the previous integral equation is obtained, so the resolving matrix equation in frequency domain is built up. Thus the longitudinal currents along the wire of the structure are obtained and E-field and B-field may be computed.

APPLICATIONS

The case study concerns a typical electric power distribution (MV/LV) air-insulated substation, fed by a 20 kV equivalent ideal voltage source, as reported in fig 1. In fig. 2 the layout of the substation is schematically depicted, also including a metallic grounded cabinet containing an electronic control and measurement equipment. The model of the physical substation arrangement is constituted by a transmission line over a perfectly conductive ground. A three-phase SF_6 circuit breaker is located at the beginning of the MV bus-bar system.

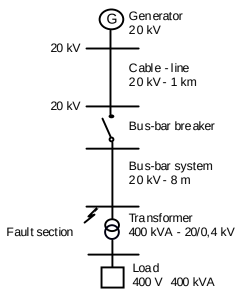

Fig. 1 - Electrical network feeding the distribution substation.

Two switching operations are considered: a) interruption of the primary currents of the MV/LV unloaded transformer; b) interruption of a three-phases fault on the primary bars of the transformer (P section of fig. 2). In case b), in the steady state condition before the fault the transformer feeds a balanced three-phase load of 400 kVA with an inductive power factor of 0.8.

The start point of opening operation is when the phase R supply voltage reaches its maximum value (16.3 kV). In both cases the simulation time is in the range around the current zero.

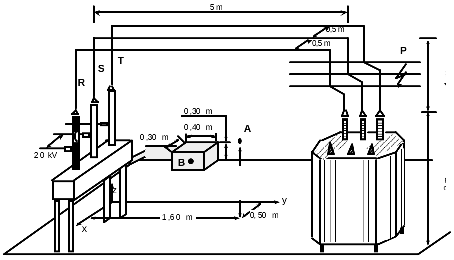

Fig. 2 - Circuit-breaker and bus-bars schematic arrangement to evaluate switching transients in two conditions: a) in interrupting primary currents of the MV/LV unloaded transformer; b) in interrupting a three-phases fault on the primary bars of the transformer (P section). A , B: fields check points.

Significant harmonic components up to 1 MHz are present in the Fourier spectrum of arc voltage and current. In order to correctly apply the DFFT algorithm, frequencies up to 500 MHz have been considered.

In calculating the electric and magnetic fields, the contribution of the power transformer has been neglected, as a first approximation.

Disconnection of the unloaded transformer

In fig. 3 and in fig. 4 calculated arc currents near current-zero and arc voltages time profiles are reported, respectively.

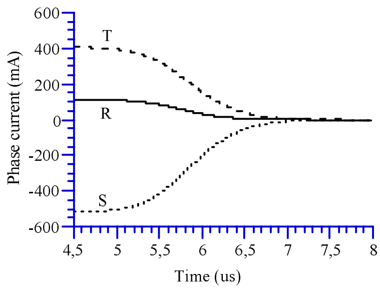

Fig. 3 - Disconnection of the unloaded transformer: calculated arc currents time profiles near current-zero.

In fig. 5 the calculated phase R arc voltage is reported in an enlarged time scale.

The simulation carried out by running the ATP-EMTP code with a time step of 1 ns, shows that no restrikes in breaker gap occurs, so the arc is extinguished at the first zero value.

In figs. 6 and 7 B_y and E_z fields time profiles are reported, as calculated in check point A of fig. 2.

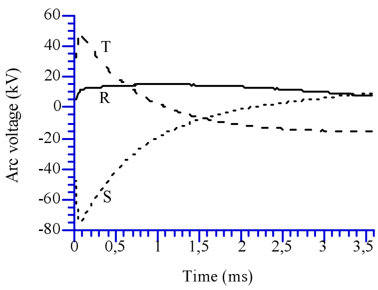

Fig. 4 - Disconnection of the unloaded transformer: calculated arc voltages time profiles.

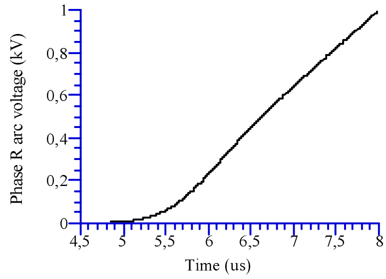

Fig. 5 - Disconnection of the unloaded transformer: calculated arc voltage time profile in enlarged scale near current-zero.

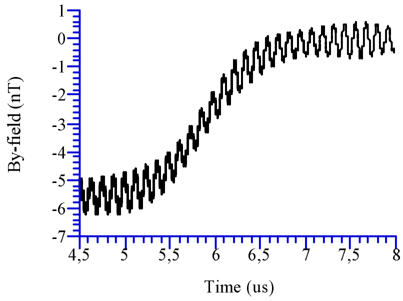

Fig. 6 - Disconnection of the unloaded transformer: By-field in A point of fig. 2.

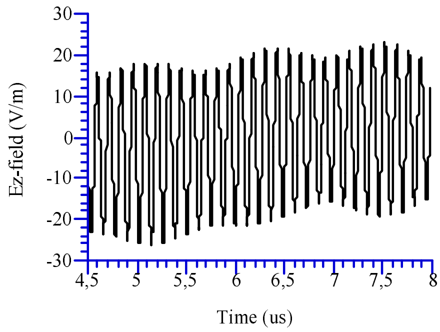

Fig. 7 - Disconnection of the unloaded transformer: Ez-field in A point of fig. 2.

Interruption of the three phase fault

In fig. 8 the calculated arc currents time profiles are reported; in fig. 9 the calculated arc current in phase R is reported for a better representation.

In figs. 10 and 11 the phase R arc voltage is shown in normal scale and in an enlarged scale, in the time range considered for the simulation, respectively.

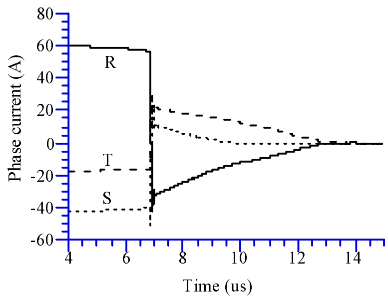

Fig. 8 - Three-phase fault in P section of fig. 2: calculated arc currents time profiles.

In figs. 14, 15 and 16 the time profiles of B_z, B_y and E_z components are reported, as calculated in check point A of fig. 2.

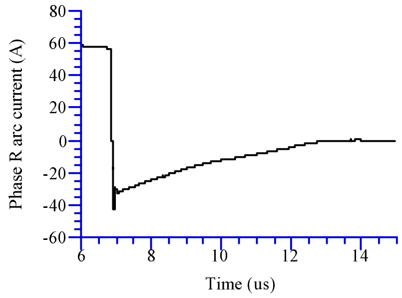

Fig. 9 - Three-phase fault in P section of fig. 2: calculated arc current time profile in enlarged scale near current-zero.

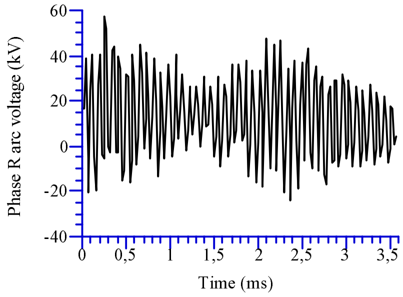

Fig. 10 - Three-phase fault in P section of fig. 2: calculated arc voltage time profile.

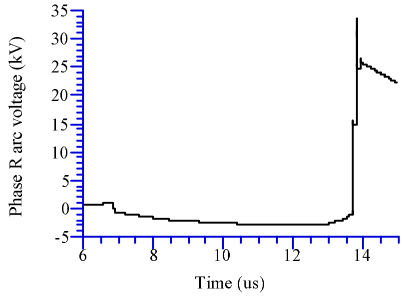

Fig. 11 - Three-phase fault in P section of fig. 2: calculated arc voltage time profile in enlarged scale near current-zero.

Fig. 8 shows that the three phase fault currents are forced to zero in a very narrow time range, but there are post arc currents before the complete arc extinction. The arc extinction causes a steep rise of the arc voltage (fig. 11).

In figs. 12 and 13 the amplitude Fourier spectra are reported for the phase R arc current and arc voltage, respectively.

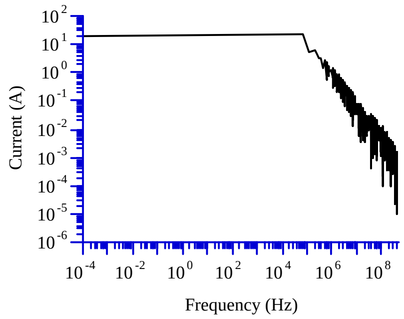

Fig. 12 - Phase R arc current: amplitude spectrum of the Fourier transform.

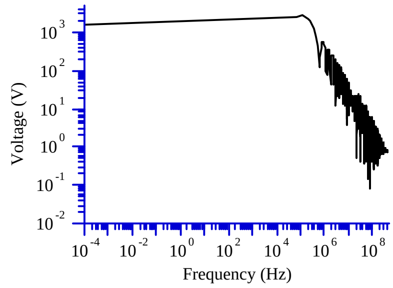

Fig. 13 - Phase R arc voltage: amplitude spectrum of the Fourier transform.

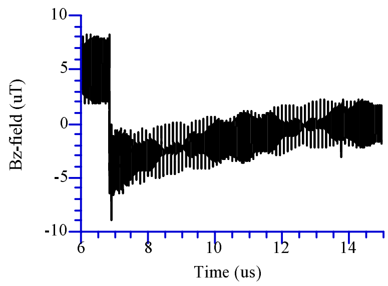

Fig. 14 - Three-phase fault in P section of fig. 2: Bz-field in A point of fig. 2.

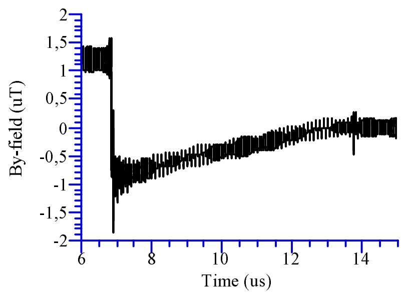

Fig. 15 - Three-phase fault in P section of fig. 2: By-field in A point of fig. 2.

The comparison of the profiles of fig. 6 and 7 with those of figs. 14, 15 and 16, related to different switching conditions, shows remarkable differences: due to relevant value of the interrupted currents, B field and E field are much higher in the case of the three phase fault; moreover, oscillations with higher peak values are present when current cross the zero value (at about 7 and 13.5 us).

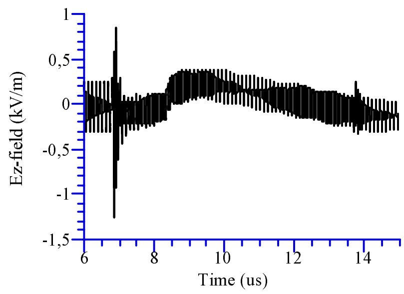

Fig. 16 - Three-phase fault in P section of fig. 2: Ez-field in A point of fig. 2.

With regard to the shielding capability of a metallic cabinet enclosing electronic devices (fig. 2), the electric field in the central point inside has been calculated without and with the metallic box simulated by means of a three dimensional wire grid structure.
In figs. 17 and 18 the E_z field time profiles, calculated in point B (fig. 2), are reported.

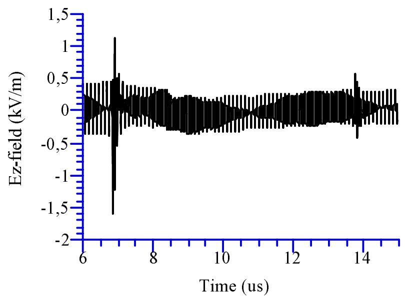

Fig. 17 - Three-phase fault in P section of fig. 2: Ez-field in B point of fig. 2 without the enclosure.

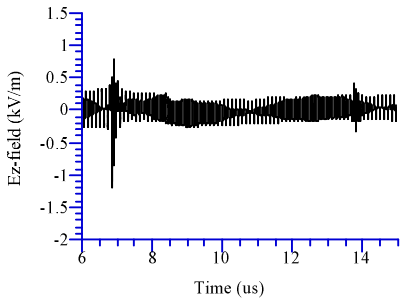

Fig. 18 - Three-phase fault in P section of fig. 2: Ez-field in B point of fig. 2 with the enclosure.

The used discretization of the metallic walls enables to estimate an attenuation of more than 25%.

CONCLUSION

In the paper, two computer codes have been used in order to characterize the electromagnetic environment of an electric power MV/LV distribution substation. The ATP-EMTP code, improved by the authors by means of a tool simulating the arc behaviour of circuit breaker, enables to predict arc currents and voltages during switching operations in common or fault conditions. Then transient electric and magnetic fields are calculated by considering the bus-bar system and arc elements as radiating antennas. To this aim, arc currents and voltages are data input in a code that uses a field approach based on the method of moments, entirely developed by the authors.
The application examples have shown the flexibility of the proposed model in order to characterize the electromagnetic environment of an electric power distribution substation and to evaluate the shielding effects of metallic cabinets enclosing equipment which are sensitive to EM noises.

REFERENCES

[1] E. Comellini et alii, "An enhanced distribution automation system based on new communication technology at ENEL", ENEL Spa, Studies and Research Directorate.

[2] C.M. Wiggins, F. S. Nickel, A. J. Haney S.E. Wright, "Measurement of switching transients in a 115 kV substation", *IEEE Trans. on Power Delivery*, vol. 4, No 1, January 1989, pp. 756-768.

[3] D.E. Thomas, C.M. Wiggins, F.S. Nickel, C.D. Ko, S.E. Wright, "Prediction of electromagnetic field and current transients in power transmission and distribution systems", *IEEE Trans. on Power Delivery*, vol. 4, no 1, January 1989, pp. 744-755.

[4] C.M. Wiggins, S.E. Wright, "Switching transients fields in substations", *IEEE Trans. on Power Delivery*, vol. 6, no 2, April 1991, pp. 591-599.

[5] B. D. Russel, S. M. Harvey, S. L. Nilsson, "Substation electromagnetic interference. Part 1: characterization and description of the transient EMI problem", *IEEE Trans. on Power Apparatus and Systems*, vol. PAS-103, No 7, July 1984, pp. 1863-1870.

[6] D. Tabara, M. Ianoz, B. Krummen, "Transient electric field in gas insulated substations and coupling with secondary cables", in *Proceedings 1998 3rd International Symposium on Electromagnetic Compatibility EMC'98 ROMA* , pp. 282-287.

[7] G.Bizjak, P.Zunko, D.Povh, "Circuit breaker model for digital simulation based on Mayr's and Cassie's differential arc equations", *IEEE Trans. on Power Delivery*, vol. 10, no 3, July 1995, pp. 1310-1315.

[8] G. Ala, P. Buccheri, M. Inzerillo, "A simulation model to predict EM radiated interference with control equipment in electric power distribution substations during switching operations", in *Proceedings 1998 3rd International Symposium on Electromagnetic Compatibility EMC'98 ROMA* , pp. 288-293.

[9] G. Ala, P. Buccheri, E. Francomano, A Tortorici, "An advanced algorithm for transient analysis of grounding systems by Moments Method", in *Proceedings 1994 IEE 2nd International Conference on Computation in Electromagnetics* ", pp. 363-366.

[10] G. Ala, P. Buccheri, "Scattering effects of large earth electrodes in the EM lightning fields", in*Proceedings 1996 8th IEEE Mediterranean Electrothecnical Conference MELECON* , pp. 827-830.

[11] G. Ala, P. Buccheri, "Coupling effects among aerial structures and earthed electrodes in a lightning protection system", in *Proceedings 1998 3rd International Symposium on Electromagnetic Compatibility EMC'98 ROMA* , pp. 360-365.